Simulation and dynamics of freeway traffic

Lino Figueiredo · J. A. Tenreiro Machado

Abstract This paper presents the new package entitled Simulator of Intelligent Transportation Systems (SITS) and a computational oriented analysis of traffic dynamics. The SITS adopts a microscopic simulation approach to reproduce real traffic conditions considering different types of vehicles, drivers and roads. A set of experiments with the SITS reveal the dynamic phenomena exhibited by this kind of system. For this purpose a modelling formalism is developed that embeds the statistics and the Laplace transform. The results make possible the adoption of classical system theory tools and point out that it is possible to study traffic systems taking advantage of the knowledge gathered with automatic control algorithms. A complementary perspective for the analysis of the traffic flow is also quantified through the entropy measure.

Keywords Intelligent transportation systems · Simulation and modelling · Traffic control · Traffic dynamics

1 Introduction

Due to the growing number of vehicles over the last five decades, we have a saturation of the transportation infrastructures. This situation affects our lives particularly in the urban areas, while people needs, more and more, to move rapidly between different places. The results are traffic congestion, accidents, transportation delays and larger vehicle pollution emissions. Several solutions were introduced to reduce these problems or their outcomes. Examples are the implementation safety systems and the construction of more and better roads and highways. Nevertheless, presently it is clear that building more roads to reduce traffic congestion is not the "right" solution, because is very expensive, while causing a considerable environmental impact, besides requiring a large space, which is an important limitation within urban areas. On the other hand, it is also straightforward that the improvement of the transport infrastructure is essential for the economical development. So, a compromise solution must be implemented [1].

The difficulties concerned with this subject motivated the research community to centre their attention in the area of ITS (Intelligent Transport Systems). This research studies the technologies and the scientific aspects with the purpose of developing new systems capable of solving some of the referred problems [2, 3].

ITS depend on results from research activities spread over many different areas such as electronics, control, communications, sensing, robotics and information systems. This multidisciplinary nature increases the problem's complexity because it requires knowledge transfer and cooperation among different research areas [4].

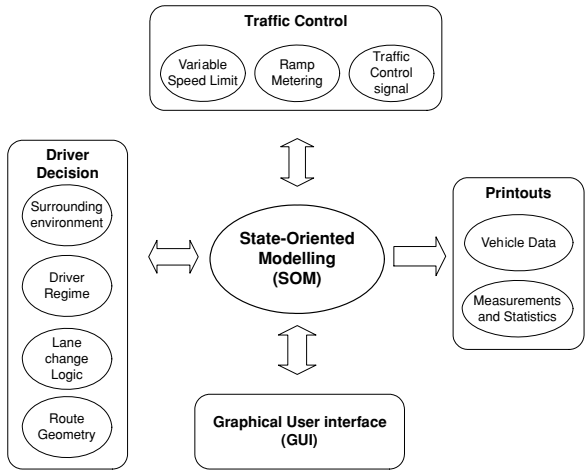

Fig. 1 SITS overall model structure

Computer simulation has become a common tool in the evaluation and development of ITS. The advantages of this tool are obvious. The simulation models can satisfy a wide range of requirements, such as: evaluating alternative treatments, testing new designs, training personnel and analyzing safety aspects [5–7].

The traffic simulation models can be classified according to various criteria, namely, the scale of independent variables, the representation of the processes and levels of detail [8]. Presently, most traffic system simulation applications are microscopic in nature and based on the simulation of vehicle–vehicle interactions [9].

The main modelling components of a microscopic traffic simulation model are: an accurate representation of the road network geometry, a detailed modelling of individual vehicles behaviour and an explicit reproduction of traffic control plans. The recent evolution of microscopic simulators has taken advantages of the state-of-the-art in the development of object-oriented simulators and graphical user interfaces.

In this line of thought, this study presents a new package for traffic simulation (SITS – Simulator of Intelligent Transportation Systems), the treatment of the data generated through a modelling formalism that embeds statistics and Laplace transform and a dynamical analysis adopting the tools of system theory and fractional calculus.

Bearing these facts in mind, this paper is organized as follows. Section 2 describes the development of the microsimulation package SITS. Section 3 presents simulation results related with the dynamics and control of a traffic system. Finally, Section 4 outlines the conclusions and the perspectives towards future research.

2 The SITS simulation package

SITS is a software tool based on a microscopic simulation approach, which reproduces real traffic conditions. The program provides a detailed modelling of the traffic network, distinguishing between different types of vehicles and drivers and considering a wide range of network geometries. SITS uses a flexible structure that allows the integration of simulation facilities for any of the ITS related areas. This new simulation package is an object-oriented implementation written in C^{++}. The overall model structure is represented on Fig. 1.

SITS models each vehicle as a separate entity in the network according to the state diagram shown in Fig. 2. Therefore, are defined five states 1 – acceleration, 2 – braking, 3 – cruise speed, 4 – stopped, 5 – collision that represent the possible vehicle states in a traffic systems.

In the novel State-Oriented Modelling (SOM) structure [10], every single vehicle in the network has one possible state for each sampling period. The transition between each state depends on the driver behaviour model and its surrounding environment. Some transitions are not possible; for instance, it is not possible to move from state #4 (stopped) to state #2 (braking), although it is possible to move from state #2 to state #4.

Included on the most important elements of SITS are the network components, travel demand, and driving decisions. Network components include the road

Fig. 2 SITS state diagram

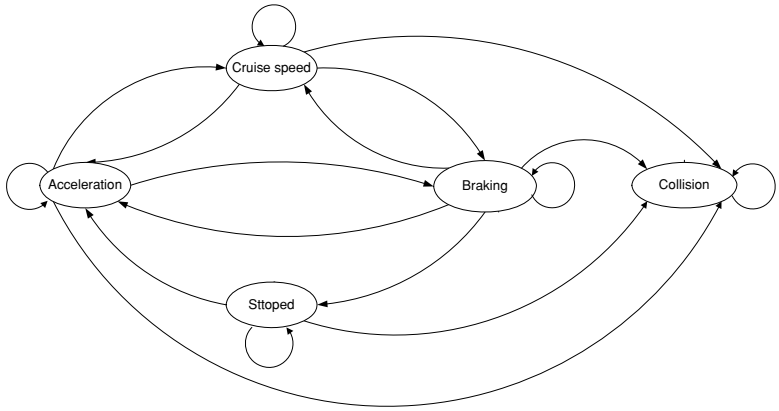

network geometry, vehicles and the traffic control. Each driver is assigned a set of attributes that describe the driver's behaviour, including desired speed, and his profile (e.g., from conservative to aggressive). Likewise, vehicles have their own specifications, including size and acceleration capabilities. Travel demand is simulated using origin destination matrices given as an input to the model.

At this stage of development the SITS considers different types of driver behaviour models, namely car following, free flow and lane changing logic. SITS considers each vehicle in the network to be in one of two driver regimes: free flow and car-following. The free flow regime prevails when there is either (i) no lead vehicle in front of the subject vehicle or (ii) the leading vehicle is sufficiently far ahead that it does not influence the subject vehicles behaviour. In the free flow case the driver travels at his desired maximum speed. Car-following regime dictates acceleration/deceleration decisions when a leading vehicle is near enough to the subject vehicle in order to maintain a safe following distance. Accelerations and decelerations are simulated using the Perception-Driver Model (PDM) [11]. According with the PDM, the driver decides to decelerate/accelerate depending on two factors: the difference between the distance to the leading vehicle and the critical distance, and his active state. The critical distance $d_{c,n}$ is defined as follows:

$$d_{c,n} = d_{sb,n} + d_{f,n} + L_{n+1} \tag{1}$$

where $d_{sb,n}$ is the safety braking distance for the vehicle n, $d_{f,n}$ is the following distance for the vehicle n, L_{n+1} is the length of the leading vehicle.

The safety braking distance $d_{sb,n}$ is given by

$$d_{sb,n} = -\frac{(v_{n+1} - v_n)^2}{2(a'_n - s_{n+1})} \tag{2}$$

where v_n is the current speed of vehicle n. v_{n+1} is the current speed of leading vehicle $n+1$. a'_n is the deceleration of vehicle n, and s_{n+1} is the deceleration/acceleration of the leading vehicle $n+1$.

The driver reduces the speed by applying a deceleration a'_n. The model relates the vehicle performances with the driver characteristics.

$$a'_n = a'_{\max,c}\, \gamma_d \tag{3}$$

where $a'_{\max,c}$ is the maximum deceleration for a vehicle of type c, and γ_d is a parameter for driver type d ($0.1 < \gamma_d < 1.0$).

The value of γ_d can be changed at any time in order to prevent a collision. This parameter defines the driver profile (e.g., from conservative $\gamma_d = 0.1$ up to aggressive $\gamma_d = 1.0$).

The value of the deceleration/acceleration s_{n+1} depends on the state of the leading vehicle. If the vehicle is in state #2 then s_{n+1} is given by Equation (3); otherwise if it is in state #1, s_{n+1} is given by Equation (4). Therefore, $s_{n+1} = 0$ only when the vehicle is in one of the other states.

$$s_{n+1} = a_{\max,c}\, \gamma_d \tag{4}$$

where $a_{\max,c}$ is the maximum acceleration for a vehicle of type c.

The following distance d_f depends on the speed of vehicle n and the associated driver profile,

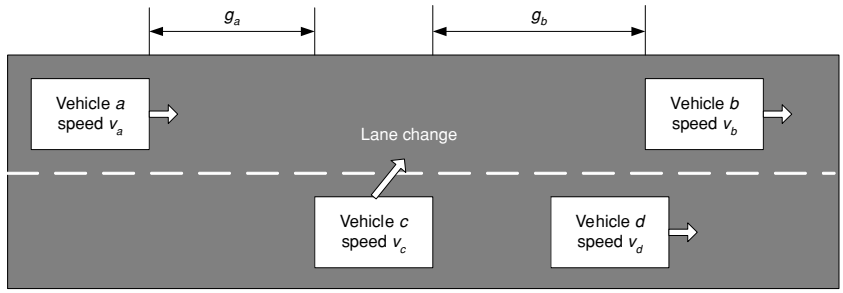

Fig. 3 Lead g_b and lag g_a gaps for a lane change manoeuvre of vehicle n

yielding:

$$d_f = v_n^2 \gamma_d \tag{5}$$

The lane changing model in SITS uses a methodology that tries to mimic a driver behaviour when producing a lane change. This methodology was implemented in three steps: (i) decision to consider a lane change; (ii) selection of a desired lane; (iii) execution of the desired lane change if the gap distances are acceptable. A driver produces a lane change manoeuvre in order to increase speed, to overtake a slower vehicle or to avoid the lane connected to a ramp. After selecting a lane, the driver examines the lead g_b and lag g_a gaps in the target lane in order to determine if the desired change can be executed, as shown in Fig. 3.

If g_a and g_b are higher than the critical distances between vehicle a and c, and c and b, respectively, then the desired lane change is executed in a single simulation sampling interval Δt.

SITS allows also the analysis of signal control devices and different road geometries considering road junctions and access ramps.

The simulation model adopted in the SITS is a stochastic one. Some of the processes include random variables such as, individual vehicle speed and input flow. These values are generated randomly according to a pre-defined amplitude interval.

The main types of input data to the simulator are the network description, the drivers and vehicles specifications and the traffic conditions. The output of SITS consists not only in a continuously animated graphical representation of the traffic network but also the data gathered by the detectors, originating different types of printouts.

SITS tracks the movements of individual vehicles to a resolution of $\Delta t = 10^{-2}$ s and uses five different colours to represent the individual vehicle states; namely, stopped (red), acceleration (green), breaking (yellow), cruise speed (blue) and collision (black).

3 Dynamics and control

3.1 Dynamics analysis

In the dynamical analysis systems theoretical tools are applied. In this line of thought, a set of simulation experiments are developed in order to estimate the influence of the vehicle speed $v(t; x)$, the road length l and the number of lanes n_l in the traffic flow $\phi(t; x)$ at time t and road coordinate x. For a road with n_l lanes the Transfer Function (TF) between the flow measured by two sensors is calculated by the expression:

$$G_{r,k}(s; x_j, x_i) = \Phi_r(s; x_j)/\Phi_k(s; x_i) \tag{6}$$

where $k, r = 1, 2, \ldots, n_l$ define the lane number, x_i and x_j represent the road coordinates ($0 \leq x_i \leq x_j \leq l$), respectively, and s is the Laplace variable.

The Laplace transform for each traffic flow is:

$$\Phi_r(s; x_j) = \mathscr{L}\{\phi_r(t; x_j)\} \tag{7a}$$

$$\Phi_k(s; x_i) = \mathscr{L}\{\phi_k(t; x_i)\} \tag{7b}$$

It should be noted that, traffic flow is a stochastic system but, in the sequel, it is shown that the Laplace transform can be used to analyse the system dynamics.

The first group of experiments considers a one-lane road (i.e., $k = r = 1$) with length $l = 1000$ m. Across the road are placed n_s sensors equally spaced. The first sensor is placed at the beginning of the road (i.e., at $x_i = 0$) and the last sensor at the end (i.e., at $x_j = l$). Therefore, we calculate the TF between two traffic flows at the beginning and the end of the road such that, $\phi_1(t; 0) \epsilon$ [0.12, 1] vehicles s^{-1} for vehicle speed

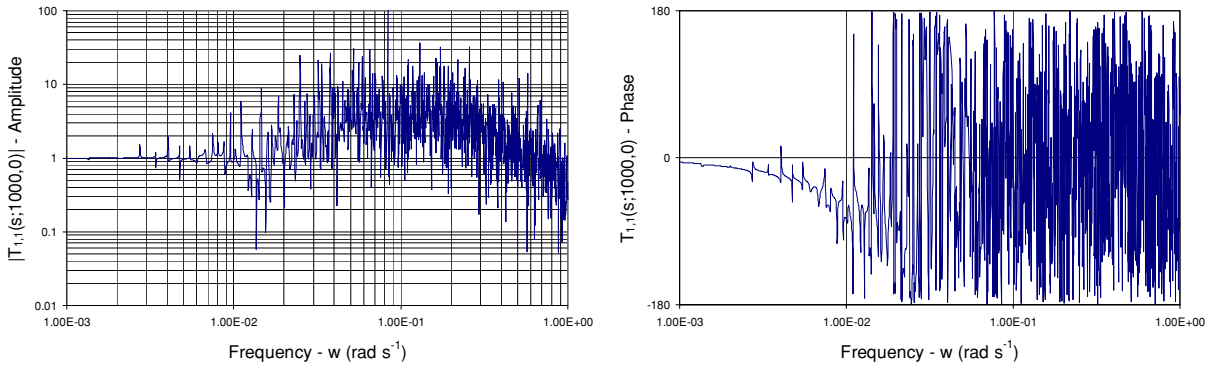

Fig. 4 (a) Amplitude diagram and (b) Phase diagram TF for $n = 1$ experiment, with $\phi_1(t;0) \epsilon$ [0.12, 1] vehicles s^{-1} and $v_1(t;0) \epsilon$ [30, 70] km h^{-1} ($v_{av} = 50$ km h^{-1}, $\Delta v = 20$ km h^{-1}, $l = 1000$ m and $n_l = 1$)

$v_1(t;0) \epsilon$ [30, 70] km h^{-1}, that is, for $v_1(t;0) \epsilon [v_{av} - \Delta v, v_{av} + \Delta v]$, where $v_{av} = 50$ km h^{-1} is the average vehicle speed and $\Delta v = 20$ km h^{-1} is the maximum speed variation. These values are generated according to a uniform probability distribution function.

The results obtained of the amplitude and phase diagram for the TF $G_{1,1}(s; 1000,0) = \Phi_1(s; 1000)/\Phi_1(s; 0)$ between the traffic flow at the beginning and end of the one-lane road is distinct from those usual in systems theory revealing a large variability (Fig. 4). Moreover, due to the stochastic nature of the phenomena involved different experiments using the same input range parameters result in different TFs (for simplicity, the phase diagram is depicted in the interval $[-180^\circ, 180^\circ]$).

This phenomenon makes the analysis complex and experience demonstrates that efficient tools that are capable of rendering clear results are still lacking. Moreover, classical models are adapted to "deterministic" tasks, and are not well adapted to the "random" operation that occurs in systems with a non-structured and changing environment.

In order to overcome the problems, alternative concepts are required. Statistics is a mathematical tool that is well adapted to handle a large volume of data, but is not capable of dealing with time-dependent relations. Therefore, to overcome the limitations of statistics, a new method is adopted, that takes advantage of the Laplace transform by embedding both tools [10].

In this line of thought, the first stage of the new modelling formalism starts by comprising a set of input variables that are free to change independently (ivs) and a set of output variables that depend on the previous ones (ovs). In a traffic system the ivs and ovs are defined as $\phi_k(x_i, t)$ and $\phi_k(x_j, t)$; that is, the traffic flow at positions x_i and x_j, respectively, at time t and for the kth lane ($k = 1, 2, 3 \ldots$).

The second stage of the formalism consists on embedding the statistical analysis into the Laplace transform through the algorithm:

(i) A statistical sample is obtained by carrying out a large number (n) of experiments having appropriate time/space evolutions. All the ivs and ovs are calculated and sampled in the time domain.
(ii) The Laplace transform is computed for each of the ivs and ovs.
(iii) Statistical indices are calculated for the Laplace spectra obtained in (ii).
(iv) The values of the statistical indices calculated in (iii) (for all the variables and for each frequency) are collected on a "composite" frequency response entitled Statistical Transfer Function (STF) of the TF.

The previous procedure may be repeated for different numerical parameters (e.g., traffic flow, vehicle speed, road geometry) and the partial conclusions integrated in a broader paradigm.

To illustrate the proposed modelling concept (STF), the simulation was repeated for a sample of $n = 2000$ and it was observed the existence of a convergence of the STF (using the median), $T_{1,1}$ (s; 1000,0), as shown in Fig. 5, for a one-lane road with length $l = 1000$ m $\phi_1(t;0) \epsilon$ [0.12, 1] vehicles s^{-1} and $v_1(t;0) \epsilon$ [30, 70] km h^{-1} (for simplicity, the phase diagram is depicted in the interval $[-180^\circ, 180^\circ]$).

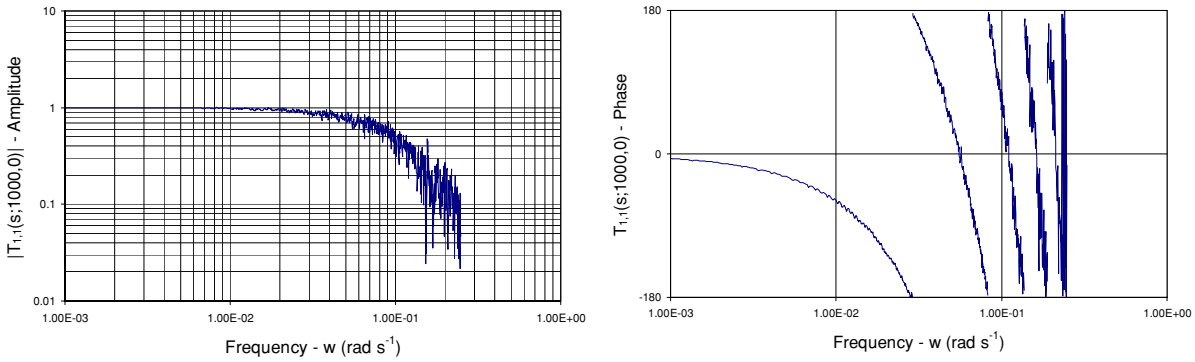

Fig. 5 Median of (a) Amplitude diagram and (b) Phase diagram TF for $n = 2000$ experiments, with $\phi_1(t;0) \epsilon$ [0.12, 1] vehicles s^{-1} and $v_1(t;0) \epsilon$ [30, 70] km h^{-1} ($v_{av} = 50$ km h^{-1}, $\Delta v = 20$ km h^{-1}, $l = 1000$ m and $n_l = 1$)

The chart has characteristics similar to those of a low-pass filter with time delay, common in systems involving transport phenomena. Nevertheless, in our case, we need to include the capability of adjusting the description to the continuous variation of the system working conditions. This requirement precludes the adoption of the usual integer-order low-pass filter and points out the need for the adoption of a fractional-order TF [12, 13]. Therefore, in this case we adopt a fractional-order system [14, 15] with time delay:

$$T_{1,1}(s;1000,0) = \frac{k_B e^{-\tau s}}{\left(\frac{s}{p}+1\right)^{\alpha}} \tag{8}$$

With this description we get not only a superior adjustment of the numerical data, impossible with the discrete steps in the case of integer-order TF, but also a mathematical tool more adapted to the dynamical phenomena involved. For fitting (8) with the numerical data it is adopted a two-step method based on the minimization of the quadratic error. In the first phase the parameters (k_B, p, α) are obtained through error amplitude minimization of the Bode diagram. Once established (k_B, p, α) in a second phase, the parameter τ is estimated through the error minimization in the Polar diagram.

For the numerical parameters of Fig. 5, we get $k_B = 1.0$, $\tau = 96.0$ s, $p = 0.07$ and $\alpha = 1.5$.

The parameters (τ, p, α) vary with the average speed v_{av} and its range of variation Δv, the road length l and the input vehicle flow ϕ_1. For example, Fig. 6 shows (τ, p, α) versus Δv (with $v_{av} = 50$ km h^{-1}) and v_{av} (with $\Delta v = 20$ km h^{-1}).

It is interesting to note in Fig. 6(a) that $(\tau, p) \rightarrow (\infty, 0)$, when $\Delta v \rightarrow v_{av}$, and $(\tau, p) \rightarrow (l v_{av}^{-1}, \infty)$, when $\Delta v \rightarrow 0$. These results are consistent with our

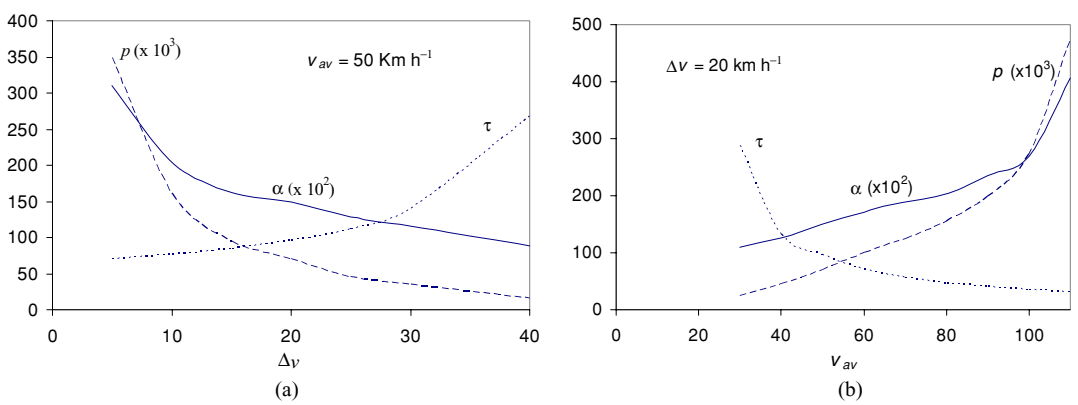

Fig. 6 Parameters τ, p and α with $n_l = 1$, $l = 1000$ m and $\phi_1(t;0) \epsilon$[0.12, 1] vehicles s^{-1} versus (a) Δv (with $v_{av} = 50$ km h^{-1}) and (b) v_{av} (with $\Delta v = 20$ km h^{-1})

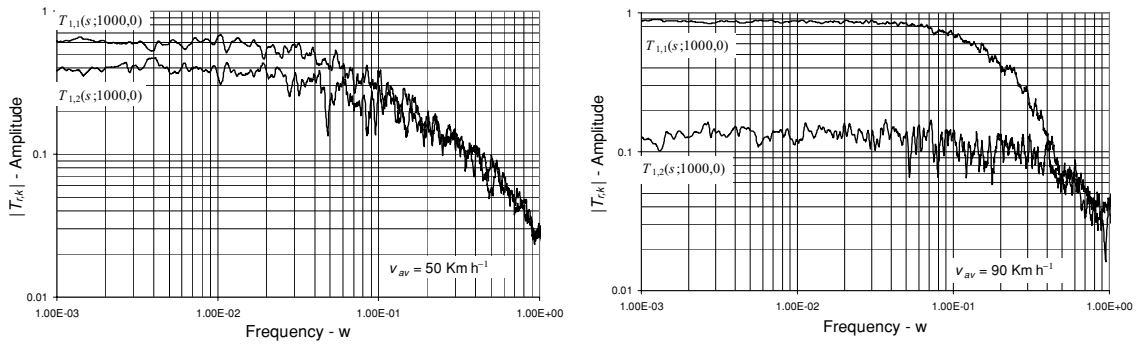

Fig. 7 Median of Bode diagram of $T_{r,k}(s;\ 1000{,}0)$ for (a) $v_{av} = 50$ km h^{-1} and (b) $v_{av} = 90$ km h^{-1}, $n_l = 2$, $l = 1000$ m, $\phi_k(t;0) \epsilon\ [0.12, 1]$ vehicles s^{-1}, $\Delta v = 20$ km h^{-1}, $k = 1, 2$

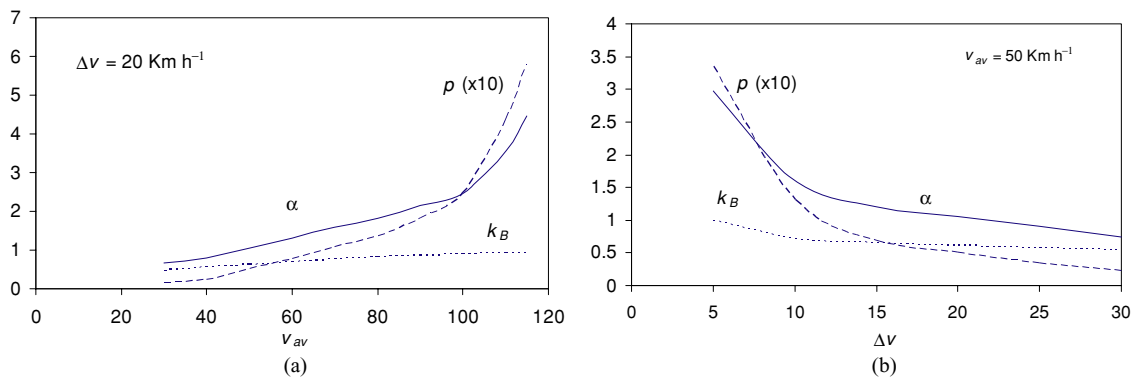

Fig. 8 Parameters (k_B, p, α) versus (a) v_{av} and (b) Δv, for $T_{1,1}(s;\ 1000{,}0)$ with $n_l = 2, l = 1000$ m and $\phi_1(t;0) \epsilon\ [0.12, 1]$ vehicles s^{-1}

experience that suggests a pure transport delay $T(s) \approx e^{-\tau s}$ ($\tau = l\ v_{av}^{-1}$), $\Delta v \to 0$ and $T(s) \approx 0$, when $\Delta v \to v_{av}$ (because of the existence of blocking cars, with zero speed, on the road). In the case of Fig. 6(b) we have $(\tau,\ p) \to (\infty, 0)$, when $v_{av} \to \Delta v$, and $(\tau,\ p) \to (0, \infty)$, when $v_{av} \to \infty$, which has a similar intuitive interpretation.

In a second group of experiments are analyzed the characteristics of the STF matrix for roads with several lanes considering identical traffic conditions (i.e., $\phi_k(t;0) \epsilon\ [0.12, 1]$ vehicles s^{-1}, $k = 1, 2$, $l = 1000$, $\Delta v = 20$ km h^{-1}, $n_l = 2$). Figure 7(a) depicts the amplitude Bode diagram of $T_{1,1}(s;\ 1000{,}0)$ and $T_{1,2}(s;\ 1000{,}0)$ for $v_{av} = 50$ km h^{-1} (i.e., $v_k(t;0) \epsilon\ [30, 70]$ km h^{-1}).

We verify that $T_{1,1}(s;1000,0) \approx T_{2,2}(s;1000,0)$ and $T_{1,2}(s;1000,0) \approx T_{2,1}(s;1000,0)$. This property occurs because SITS uses a lane change logic where, after the overtaking, the vehicle tries to return to the previous lane. Therefore, lanes 1 and 2 have the same characteristics leading to identical STF.

Figure 7(b) presents the amplitude Bode diagram of $T_{1,1}(s;\ 1000{,}0)$ and $T_{1,2}(s;\ 1000{,}0)$ for $v_{av} = 90$ km h^{-1} (i.e., $v_k(t;0) \epsilon\ [70, 110]$ km h^{-1}).

Comparing Fig. 7(a) and these results, we conclude that the transfer matrix elements vary significantly with v_{av}. Moreover, the STF parameter dependence is similar to the one-lane case represented previously [16]. Figure 8(a) and (b) show the variation of parameters (k_B, p, α) for $T_{1,1}(s;\ 1000{,}0)$ versus v_{av} (with $\Delta v = 20$ km h^{-1}) and Δv (with $v_{av} = 50$ km h^{-1}), respectively, for $n_l = 2$.

Figure 9(a) and (b) show the amplitude Bode diagrams of $T_{1,1}$, $T_{1,2}$, $T_{1,3}$, and $T_{2,1}$, $T_{2,2}$, $T_{2,3}$, for a road with $n_l = 3$ and $l = 1000$ m.

For the same reasons we verify that $T_{1,1}(s;\ 1000,\ 0) \approx T_{3,3}(s;\ 1000,\ 0)$, $T_{1,2}(s;\ 1000,\ 0) \approx T_{3,2}(s;\ 1000,\ 0)$ and $T_{1,3}(s;\ 1000,\ 0) \approx T_{3,1}(s;\ 1000,\ 0)$.

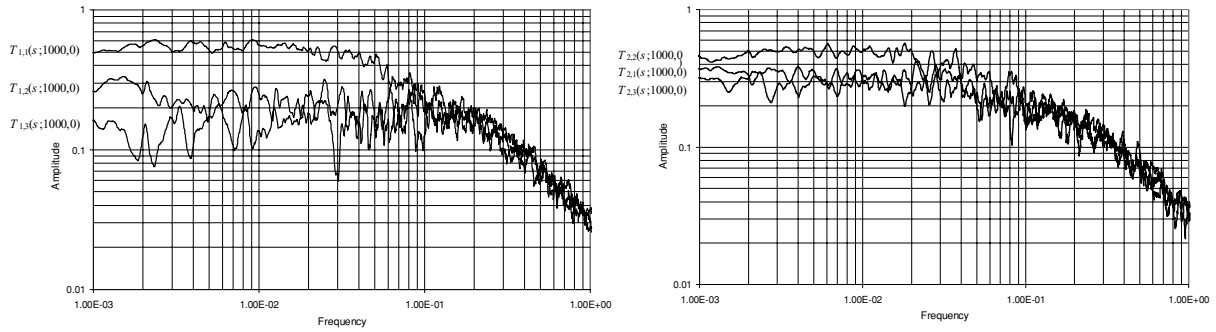

Fig. 9 Median of Bode diagram of (a) $T_{1,k}(s;\ 1000{,}0)$ and (b) $T_{2,k}(s;\ 1000{,}0)$, $n_l = 3$, $l = 1000$ m, $\phi_k(t;0) \epsilon\ [0.12,\ 1]$ vehicles s^{-1}, $v_{av} = 50$ km h^{-1}, $\Delta v = 20$ km h^{-1}, $k = 1, 2, 3$

Fig. 10 Overall traffic control concept

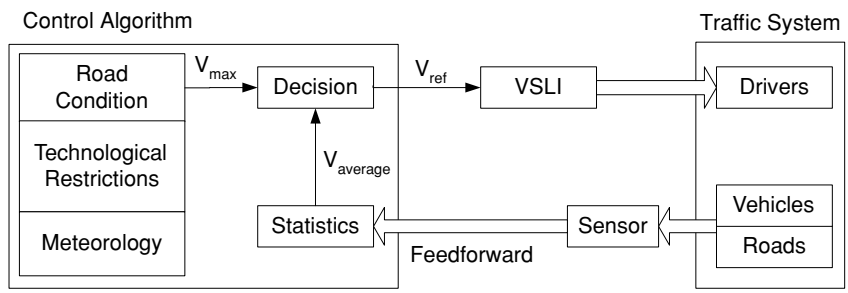

We conclude that

(i) The time delay τ is independent of the number of lanes n_l (considering the same input flow $\phi_1(t;0)$).
(ii) For a fixed set of parameters we have for each STF gain $\times$ bandwidth $\approx$ constant.
(iii) For each row of the transfer matrix, the sum of the STF gains is the unit.
(iv) The gains and the poles of the diagonal elements of the STF matrix are similar. The gain of the non-diagonal elements, that represent dynamic coupling between the lanes, are lower (due to iii), but the corresponding pole are higher (due to ii).
(v) The fractional order α increases with v_{av}. Nevertheless, the higher the number of lanes the lower the low-pass filter effect, that is, the smaller the value of α.

3.2 Traffic control

Based on the previous dynamic description, in this section we evaluate a new concept for traffic control (Fig. 10). In this perspective, it is adopted a Variable Speed Limit Indicator (VSLI) to control the vehicle speed. This kind of control scheme leads to a homogenization of traffic flow (i.e., to a more uniform car speed within a lane and of average speeds on different lanes) which is believed to reduce the risk of falling into congestion at high traffic densities and to increase the freeways capacity [17, 18].

The reference speed v_{ref} is displayed by the VSLI, at a given position x_{VSLI}, while a Feedforward Sensor (FS) is placed at distance x_{FS} ahead of the VSLI. Figure 11 shows the traffic control system adopted.

The reference speed is given by

$$v_{\text{ref}} = \rho v_{\max} + (1 - \rho) v_{\text{average}}, \quad 0 < \rho < 1 \tag{9}$$

where $v_{\max}$ is the maximum speed allowed in the lane, v_{average} is the average traffic speed of the FS readings.

Therefore, in the viewpoint of control theory v_{ref} consists on the 'reference signal', v_{average} is the 'feedforward' and Equation (9) is the 'controller'.

In the experiments we have $x_{\text{VSLI}} = 200$ m, $x_{\text{FS}} = 5$ m, $l = 1000$ m, $n_l = 1$, $v_{\max} = 100$ km h^{-1}, $\rho = 0.5$ and the speed limit displayed by the VSLI is computed with a sampling interval $T_s = 100$ s.

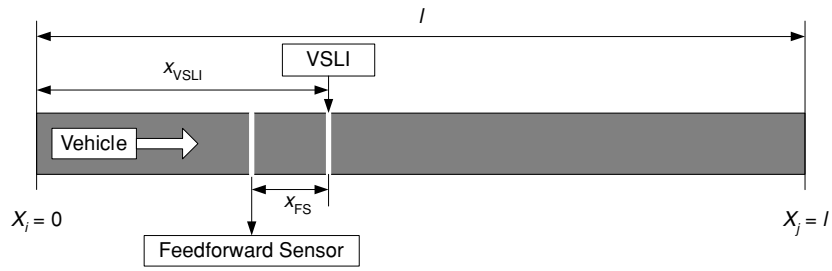

Fig. 11 Traffic control system adopted

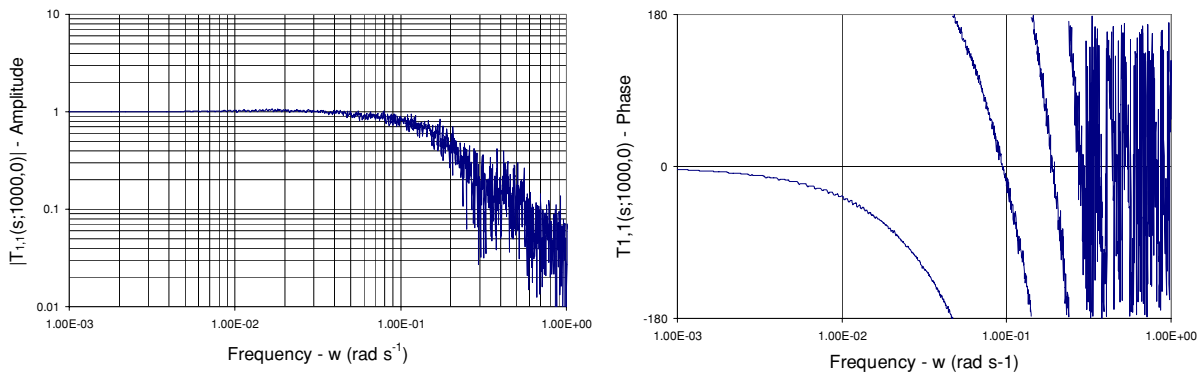

(a) (b)

Fig. 12 Median of Polar diagram of the STF $T_{1,1}(s;\ 1000{,}0)$ for a closed-loop case with $\phi_1(t;0) \epsilon\ [0.12, 1]$ vehicles s^{-1} and $v_1(t;0) \epsilon\ [30, 70]$ km h^{-1} ($v_{av} = 50$ km h^{-1}, $\Delta v = 20$ km h^{-1}, $l = 1000$ m and $n_l = 1$)

The dynamics of the controlled system differs somehow from the previous open-loop case as can be verified in Fig. 12 (for simplicity, the phase diagram is depicted in the interval $[-180°, 180°]$). An analytical expression for the STF, fitting closely the resulting data, requires a large number of poles and zeros. In order to easy the comparison of the open and close loop dynamics, in the sequel it is adopted expression (8), since we can still get a reasonable curve fitting.

Figures 13–15 depicts the variation of the STF parameters τ, p, and α versus v_{av}, respectively, for the open loop and controlled cases, with $\Delta v = 20$ km h^{-1} and $\phi_1(t;0) \epsilon\ [0.12, 1]$ vehicles s^{-1}.

It can be observed that reducing v_{av}, for the controlled case, yields:

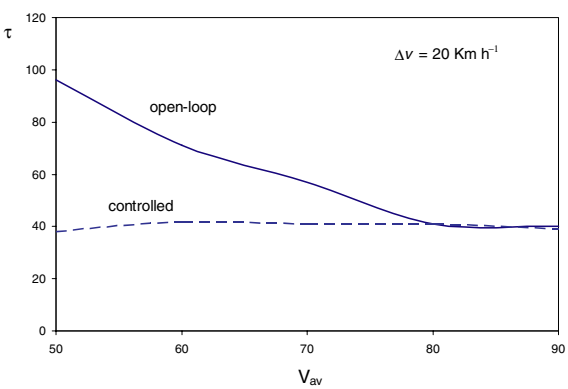

Fig. 13 Parameters τ versus v_{av} for controlled and the closed-loop cases, with $\Delta v = 20$ km h^{-1}, $n_l = 1$, $l = 1000$ m and $\phi_1(t;0) \epsilon\ [0.12, 1]$ vehicles s^{-1}

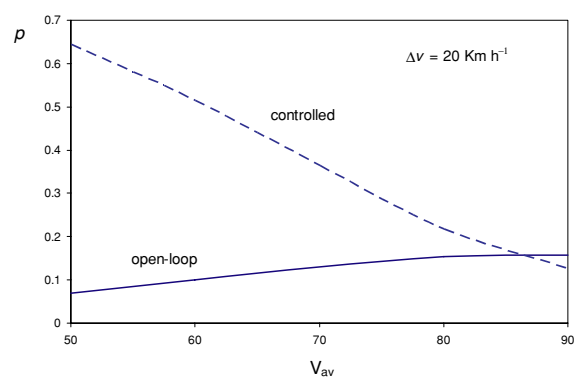

Fig. 14 Parameters p versus v_{av} for controlled and the closed-loop cases, with $\Delta v = 20$ km h^{-1}, $n_l = 1$, $l = 1000$ m and $\phi_1(t;0) \epsilon\ [0.12, 1]$ vehicles s^{-1}

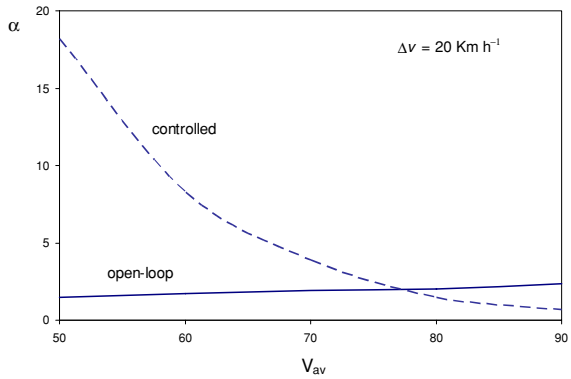

Fig. 15 Parameters α versus v_{av} for controlled and the closed-loop cases, with $\Delta v = 20$ km h^{-1}, $n_l = 1$, $l = 1000$ m and $\phi_1(t;0) \epsilon [0.12, 1]$ vehicles s^{-1}

(i) The time delay τ remains almost constant which is justified by the VSLI control effect.
(ii) The pole p increases corresponding to a larger bandwidth.
(iii) The variation of α seems to be related with the elimination of noise associated with uncontrolled (i.e., with large Δv) traffic. Nevertheless, a clear understanding of the complete phenomena is still under research.

3.3 Entropy analysis

A complementary perspective for the analysis of the traffic flow along the road can be quantified through the entropy $H(x) = N^{-1} \sum_i f_i \ln(f_i)$, where $f_i = n_i/N$, N is the total number of vehicles used in the simulation and n_i is the absolute frequency. In our experiments $N = 2048$ was adopted [19, 20].

A set of simulations analyses the variation of $H(x)$ for different ranges of vehicle speed. Figure 16 shows the results for an average vehicle speed of $v_{av} = 50$ km h^{-1} in the ranges $v_1(t;0) \epsilon [20, 80]$, $v_1(t;0) \epsilon [30, 70]$, $v_1(t;0) \epsilon [40, 60]$, $v_1(t;0) \epsilon [45, 55]$ and $v_1(t;0) \epsilon [48, 52]$ km h^{-1}. The entropy decreases along the road because the faster vehicles have to diminish their speeds to match the speed of the slower vehicles. Figure 16 also identifies two transients, namely the input and output transients.

It can be observed that, for small Δv, $H(x)$ remains almost constant and the transients are difficult to detect. This is justified by the fact that the vehicles have a small variation of speeds, which originates a minimal interference among the vehicles. Also relevant are the rise of the output transient and the convergence of entropy, for larger Δv.

In Fig. 17 it is compared the variation of the entropy $H(x)$ for roads with one and three lanes. At the beginning of the road the entropy has almost the same value for both cases; however, it is clear that for $x > 500$ m, the entropy for the one-lane road decreases faster than for the three-lanes case. This phenomenon occurs because, for a road with three-lanes, it is applied a lane change scheme that gives priority to the overtaking through the left lane. Therefore, the entropy of the right lane is lower than the entropy of the left lane.

In Fig. 18 is compared the variation of $H(x)$ for the open loop and the controlled cases. We conclude that we get a strong variation caused by the control effect of the VSLI placed at $x = 200$ m. Therefore, for $200 < x < 450$ we observe a transient, while for $x > 450$ the value of $H(x)$ remains almost constant meaning a steady-state regime with uniform vehicle speed.

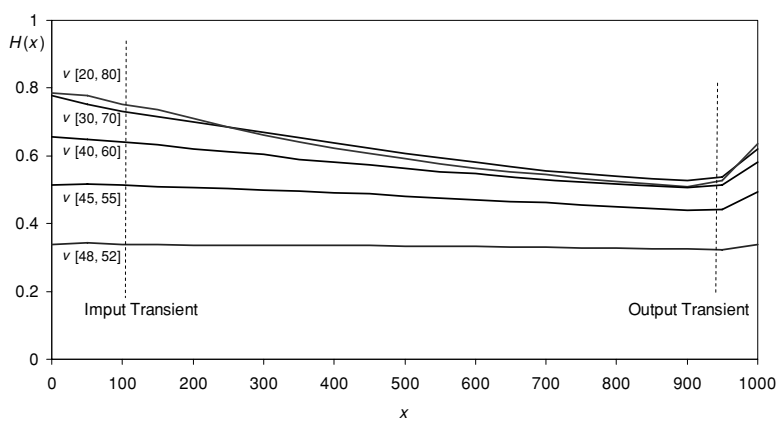

Fig. 16 Entropy $H(x)$ of the traffic velocity versus the position x for $n_l = 1$, $l = 1000$ m, $v_{av} = 50$ km h^{-1} and $\phi_1(t;0) \epsilon [0.12, 1]$ vehicles s^{-1}

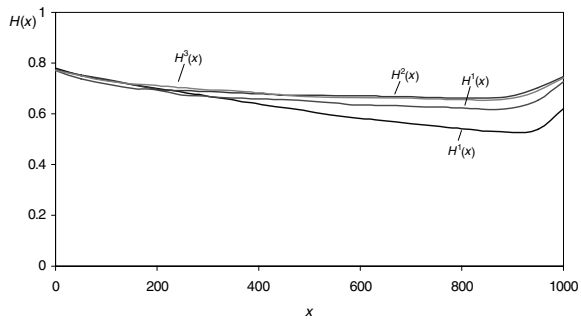

Fig. 17 Entropy $H(x)$ of the traffic velocity versus the position x for one-lane and three-lanes roads with length $l = 1000$ m and $v_1(t) \epsilon [30, 70]$ km h^{-1} and $\phi_1(t) \epsilon [0.12, 1]$ vehicles s^{-1}

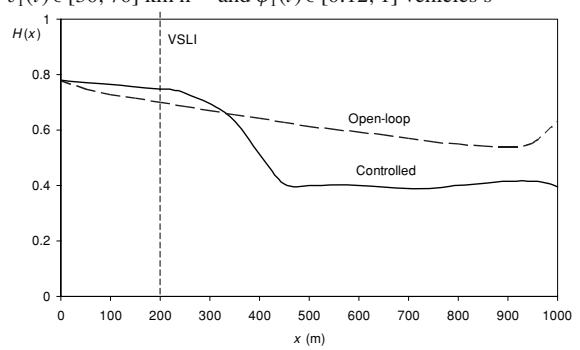

Fig. 18 Entropy $H(x)$ of the traffic velocity versus the position x for $n_l = 1$, $l = 1000$ m, $v_1(t; 0) \epsilon [30, 70]$ km h^{-1} with $\phi_1(t; 0) \epsilon [0.12, 1]$ vehicles s^{-1}

4 Conclusions

This paper described a new software tool based on a microscopic simulation approach that reproduces distinct car traffic operating conditions and several types of road networks. At this stage of development the SITS considers different types of driver behaviour model, namely car following, free flow and lane changing logic. Once established the SITS capabilities a set of simulations were then carried out in order to analyse the dynamic phenomena involved in traffic systems. The data generated by the SITS was processed by a mathematical modelling formalism based on embedding statistics into the Laplace transform. This strategy proved to be well adapted to a systems theory perspective and to a study based on the transfer function paradigm. Moreover, the description integrated implicitly the concepts of fractional calculus leading to a more natural treatment of the *continuum* of the model parameters. Motivated by the dynamical analysis a control algorithm was developed and its performance was analysed from a system theoretical viewpoint.

References

1. Figueiredo, L., Jesus, I., Machado, J., Ferreira, J., Santos, J.: Towards the development of intelligent transportation systems. In: Proceedings of the 4th IEEE Intelligent Transportation Systems Conference, Oakland, CA pp. 1207–1212 (2001)
2. Ghosh, S., Lee, T.: Intelligent transportation systems – new principles and architetures. CRC Press, Boca Raton, FL (2000)
3. Sussman, J.: Introduction to transportation systems. Artech House, Norwood, MA (2000)
4. McQueen, B., McQueen, J.: Intelligent transportation systems architectures. Artech House, Norwood, MA (1999)
5. Lieberman, E., Rathi, A.K.: Traffic simulation. In: Traffic flow theory. Oak Ridge National Laboratory, chapter 10 (1997)
6. Pursula, M.: Simulation of traffic systems – an overview. J. Geogr. Inform. Decision Anal. **3**, 1–8 (1999)
7. Nagel, K.: Particle hopping models and traffic flow theory. Phys. Rev. E **53**(5), 46–55 (1996)
8. Gerlough, D., Huber, M.: Traffic flow theory. A monograph. Transport Research Board, Washington, DC, Special Report 165 (1975)
9. Gabbard, J.F.: Car-following models. In: Papageorgiou, M. (ed.) Concise Encyclopedia of Traffic and Transportation Systems. Pergamon Press, New York (1991)
10. Figueiredo, L., Machado, J., Ferreira, J.: Dynamical analysis of freeway traffic. IEEE Trans. Intell. Transport. Syst. **5**(4), 259–266 (2004)
11. Figueiredo, L., Machado, J., Ferreira, J.: A system approach to the analysis of traffic dynamics. In: Proceedings of the IEEE International Conference on Networking, Sensing and Control, Taipei, Taiwan, pp. 249–254 (2004)
12. Oldham, K.B., Spanier, J.: The Fractional Calculus: Theory and Applications of Differentiation and Integration to Arbitrary Order. Academic Press, New York (1974)
13. Samko, S., Kilbas, A., Marichev, O.: Fractional Integrals and Derivatives: Theory and Applications. Gordon & Breach, New York (1993)
14. Podlubny, I.: Fractional Differential Equations. Academic Press, San Diego, CA (1999)
15. Tenreiro Machado, J.A.: A probabilistic interpretation of the fractional-order differentiation. FCAA-J. Fract. Calculus Appl. Anal. **6**(1), 73–80 (2003)
16. Figueiredo, L., Machado, J., Ferreira, J.: Fractional-order dynamics in freeway traffic. Int. J. Pure Appl. Math. **13**(2), 167–179 (2004)
17. Papageorgiou, M., Diakaki, C., Dinopoulou, V., Kotsialos, A., Wang, Y.: Review of road traffic control strategies. Proc. IEEE **91**(12) (December 2003)
18. Smulders, S.: Control of freeway traffic flow by variable speed signs. Transp. Res. B **24**, 111–132 (1990)
19. Abramson, N.: Information Theory and Coding. McGraw-Hill, New York (1963)
20. Figueiredo, L., Machado, J., Ferreira, J.: On the dynamics analysis of freeway traffic. In: Proceedings of the 6th IEEE Intelligent Transportation Systems Conference, Shanghai, China, pp. 358–363 (2003)